



## Get Clarity On Generics

Cost-Effective CT & MRI Contrast Agents



FRESENIUS  
KABI

WATCH VIDEO

# AJNR

This information is current as  
of August 10, 2025.

## Imaging Characteristics of CNS Neuroblastoma- *FOXR2*: A Retrospective and Multi-Institutional Description of 25 Cases

A. Tietze, K. Mankad, M.H. Lequin, L. Ivarsson, D. Mirsky,  
A. Jaju, M. Kool, K.V. Hoff, B. Bison and U. Löbel

*AJNR Am J Neuroradiol* published online 22 September  
2022

<http://www.ajnr.org/content/early/2022/09/22/ajnr.A7644>

# Imaging Characteristics of CNS Neuroblastoma-FOXR2: A Retrospective and Multi-Institutional Description of 25 Cases

 A.Tietze,  K. Mankad,  M.H. Lequin,  L. Ivarsson,  D. Mirsky,  A. Jaju,  M. Kool,  K.V. Hoff,  B. Bison, and  U. Löbel



## ABSTRACT

**BACKGROUND AND PURPOSE:** The 5th edition of the World Health Organization Classification of CNS tumors defines the CNS neuroblastoma *FOXR2* in the group of embryonal tumors. Published clinical outcomes tend to suggest a favorable outcome after resection, craniospinal irradiation, and chemotherapy. This multicenter study aimed to describe imaging features of CNS neuroblastoma-*FOXR2*, which have been poorly characterized thus far.

**MATERIALS AND METHODS:** On the basis of a previously published cohort of tumors molecularly classified as CNS neuroblastoma-*FOXR2*, patients with available imaging data were identified. The imaging features on preoperative MR imaging and CT data were recorded by 8 experienced pediatric neuroradiologists in consensus review meetings.

**RESULTS:** Twenty-five patients were evaluated (13 girls; median age, 4.5 years). The tumors were often large (mean, 115 [SD, 83] mL), showed no (24%) or limited (60%) perilesional edema, demonstrated heterogeneous enhancement, were often calcified and/or hemorrhagic (52%), were always T2WI-hyperintense to GM, and commonly had cystic and/or necrotic components (96%). The mean ADC values were low ( $687.8 [SD 136.3] \times 10^{-6} \text{ mm}^2/\text{s}$ ). The tumors were always supratentorial. Metastases were infrequent (20%) and, when present, were of nodular appearance and leptomeningeal.

**CONCLUSIONS:** In our cohort, CNS neuroblastoma *FOXR2* tumors showed imaging features suggesting high-grade malignancy and, at the same time, showed characteristics of less aggressive behavior. There are important differential diagnoses, but the results of this study may assist in considering this diagnosis preoperatively.

**ABBREVIATIONS:** ATRT = atypical teratoid/rhabdoid tumors; CNS NB-*FOXR2* = CNS neuroblastoma *FOXR2*-activated; CNS-PNET = primitive neuroectodermal tumors of the CNS; ETMR = embryonal tumor with multilayered rosettes; ITD = internal tandem duplication; WHO = World Health Organization

In the recent 5th edition of the World Health Organization (WHO) Classification of CNS Tumors, published in 2021,<sup>1</sup> the CNS neuroblastoma *FOXR2*-activated (CNS NB-*FOXR2*) has been included as a new entity in the group of embryonal tumors

that are highly malignant CNS tumors mainly occurring in children, adolescents, or young adults.<sup>2</sup> In the 2016 update of the WHO Classification, the embryonal tumors had emerged from the primitive neuroectodermal tumors of the CNS (CNS-PNET), which were replaced after an increasing number of molecular markers and genetic alterations had substantially advanced diagnostic specificity. In their important re-analysis of previously diagnosed CNS-PNET using DNA methylation profiles, Sturm et al<sup>3</sup> were able to show that this group of tumors is highly heterogeneous, consisting of many known entities, eg, medulloblastoma, embryonal tumor with multilayered rosettes (ETMR), or atypical teratoid/rhabdoid tumors (ATRT) among others. In

Received March 28, 2022; accepted after revision July 27.


From the Institute of Neuroradiology (A.T.) and Department of Pediatric Oncology and Hematology (K.V.H.), Charité—Universitätsmedizin Berlin, corporate member of Freie Universität Berlin and Humboldt-Universität zu Berlin, Berlin, Germany; Department of Radiology (K.M., U.L.), Great Ormond Street Hospital, London, UK; Department of Radiology (M.H.L.), University Medical Center Utrecht, Utrecht, the Netherlands; Department of Pediatric Radiology (L.I.), Queen Silvias Children's Hospital, Sahlgrenska University Hospital, Gothenburg, Sweden; Department of Pediatric Radiology and Imaging (D.M.), Children's Hospital Colorado, Denver, Colorado; Department of Medical Imaging (A.J.), Ann and Robert H. Lurie Children's Hospital of Chicago, Chicago, Illinois; Hopp Children's Cancer Center (M.K.), Heidelberg, Germany; Division of Pediatric Neurooncology (M.K.), German Cancer Research Center and German Cancer Consortium, Heidelberg, Germany; Princess Máxima Center for Pediatric Oncology (M.K.), Utrecht, the Netherlands; and Department of Neuroradiology (B.B.), University Hospital Augsburg, Augsburg, Germany.


A. Tietze and K. Mankad shared first authorship.

B. Bison and U. Löbel shared last authorship.

This work was supported by the German Research Foundation (DFG, SFB295RETUNE).

Please address correspondence to Anna Tietze, MD, Institute of Neuroradiology, Charité—Universitätsmedizin Berlin, corporate member of Freie Universität Berlin and Humboldt-Universität zu Berlin, Augustenburger Platz 1, D. 13353 Berlin, Germany; e-mail: anna.tietze@charite.de

 Indicates open access to non-subscribers at [www.ajnr.org](http://www.ajnr.org)

 Indicates article with online supplemental data.

<http://dx.doi.org/10.3174/ajnr.A7644>

addition, DNA methylation analyses revealed several new tumor types in this group, one of which is the CNS NB-*FOXR2*.

Available clinical data so far suggest that favorable rates of overall survival can be achieved for patients with CNS NB-*FOXR2* when treated with surgical resection, craniospinal irradiation, and chemotherapy.<sup>4,5</sup> Imaging characteristics suggesting the diagnosis are currently based on the description of single patients,<sup>6,7</sup> and to the best of our knowledge, larger series are not yet available. The reason is undoubtedly the increasingly detailed tumor classification, which results in a low incidence of confirmed cases in single centers and makes international collaboration essential to pool imaging data.

The aim of this article was to describe the imaging characteristics of CNS NB-*FOXR2* based on an international patient cohort and, at the same, establish a practical approach to collect and evaluate larger series across multiple centers.

## MATERIALS AND METHODS

The cohort is based on a previously published cohort of pathology samples with the original diagnosis of CNS-PNET, which was subsequently molecularly reclassified as CNS NB-*FOXR2*.<sup>4</sup> This study was evaluated and approved by the ethics board of the coordinating institutions. Molecular diagnosis was confirmed by DNA methylation classification (Version 11b4 or higher; [www.molecularneuropathology.org](http://www.molecularneuropathology.org)) in each included case.<sup>8</sup> Informed consent was obtained by the patients or legal representatives at the time of the initial study or registry inclusion, or for some centers, the requirement for informed consent was waived. Imaging data for 2 of the cases have been published previously.<sup>6</sup>

The image evaluation team consisted of at least 1 local neuroradiologist. Consensus decisions were made in joint online meetings on a weekly basis for 12 weeks regarding the following characteristics on pseudonymized images: 1) location, 2) cortical and/or WM involvement, 3) assumed tumor origin, 4) calvarial involvement, 5) approximation of volume (calculated [transverse  $\times$  craniocaudal  $\times$  anterior-posterior diameter]/2), 6) strength of enhancement compared with the choroid plexus (none, mild, intermediate, strong), 7) extent of enhancement (in categories: 0%, 0%–25%, 25%–50%, 50%–75%, 75%–100%, or 100% of the solid tumor component), 8) T2WI intensity compared with unaffected cortex, 9) susceptibility indicating calcification and/or hemorrhage on gradient-echo imaging (T2\* or SWI, potentially further specified by CT, T1WI, T2WI), 10) average  $ADC_{\text{minimum}}$ ,  $ADC_{\text{mean}}$ ,  $ADC_{\text{maximum}}$  values ( $\pm$ SD), in an ROI, 0.14–0.65 cm<sup>2</sup> in size, in visually determined areas with the lowest values, 11) multifocality, 12) multilobulated appearance, 13) the presence/extent of perifocal edema (in categories: none, < 25% of the perimeter, 25%–75%, 100%), 14) the presence of nonsolid components (thin-walled cysts and/or necrotic regions defined as having irregular and thick borders), 15) extent of nonsolid components (in categories: 0%, 0%–25%, 25%–50%, 50%–75%, 75%–100%, or 100% of solid-to-entire tumor), 16) the presence and extent of hydrocephalus (in categories: none, mild with ventricular dilation, moderate with ventricular dilation and periventricular edema, and severe with additional sulcal effacement),<sup>9</sup> and 17) laminar and/or nodular intracranial and/or spinal metastases. Results of arterial spin-labeling perfusion-weighted imaging or

MRS were reported when available. Descriptive statistics were used to describe the data including median/interquartile range for non-normally distributed data and mean (SD) for normally distributed nominal data. All other variables were reported as percentages.

## RESULTS

### Patients

MR imaging data were available for 25 treatment-naïve patients (13 girls) with CNS NB-*FOXR2* diagnosed between 2003 and 2021. The median age was 4.5 years (interquartile range, 3.1–9 years; range, 1.4–16 years).

### Imaging

MR imaging data consisted of T1WI, T2WI, FLAIR, and contrast-enhanced T1WI for all patients, gradient-echo imaging (T2\* or SWI) for 14 patients, and DWI for 21 patients. Arterial spin-labeling PWI and single-voxel MRS (short TE) were available for 1 patient. All MR images were acquired before total/partial/subtotal tumor resection or treatment initiation. In a single patient, MR imaging was performed after the insertion of an external ventricular drain; all other patients were treatment-naïve. Four patients had a baseline CT scan.

### Imaging Features

Results are summarized in the Online Supplemental Data, and representative imaging features in selected patients are shown in Fig 1. Further examples are available in the Online Supplemental Data, and all results are given as Online Supplemental Data. The brain regions most frequently affected were the frontal lobe (72%), followed by the parietal (44%) and temporal (36%) lobes, as well as the basal ganglia (32%). Typically, >1 region was involved. In most cases (80%), 1 or 2 anatomic compartments were involved, mostly the frontal lobe with or without the basal ganglia/thalami. In most cases, the tumor directly abutted the ventricular system without normal tissue seen between the tumor and the ventricular wall. Often, the ventricular wall was infiltrated (64%; Fig 1A). In 60% of cases, the right hemisphere was affected. The WM was always infiltrated. In 80% of cases, there was also infiltration of the cortex, while in 20%, the cortex was merely compressed. Generally, we found it difficult to determine the origins of the tumors owing to their large sizes, but assuming that the epicenter of the tumor usually reflects the origin, 52% appeared to originate in the WM, and 32%, in the cortex. In only 8% of cases, did the tumors seem to originate from the deep GM and/or the WM of the internal capsule. None of the cases occurred in the brainstem or the infratentorial compartment.

Calvarial remodeling was found in 48%, associated with calvarial signal changes in 33%. The average tumor size was 115 (SD, 83) mL and was often larger in the 48% of cases with associated skull remodeling and scalloping (148 [SD, 68] mL) compared with cases without remodeling (85 [SD, 87] mL; Fig 1G).

In most cases, solid tumor components showed intermediate-but-inhomogeneous enhancement as well as peripheral enhancement of necrotic elements (Fig 1E, -F) or cyst walls. Dural infiltration was noted in 2 cases.

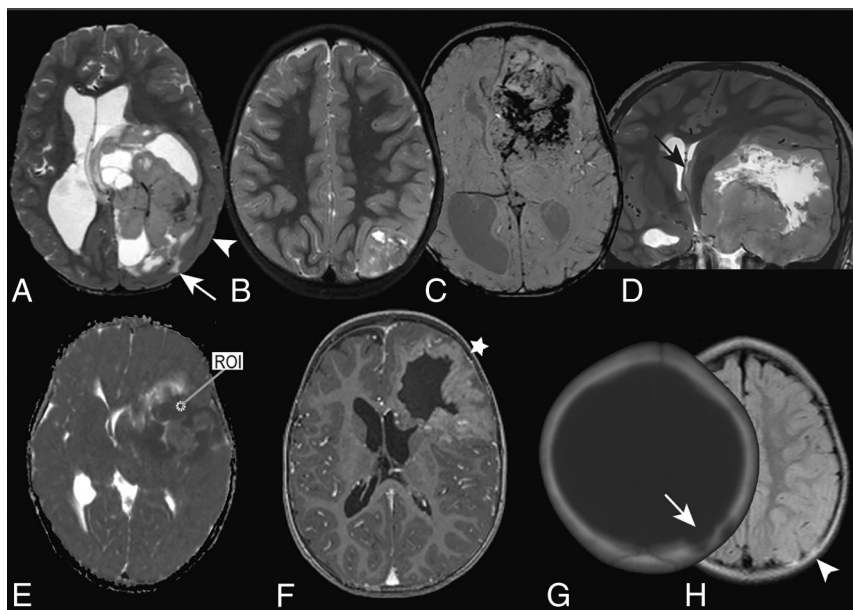


**FIG 1.** Typical imaging characteristics of CNS NB-FOXR2 in different patients (A, A 2.5-year-old girl; B, G, H, A 3-year-old girl; C, A 4.2-year-old girl; D, A 16-year-old boy; E, A 4-year-old boy; F, A 2.7-year-old boy). Most tumors were characterized by T2WI signal heterogeneity but always contained hyperintense regions compared with cortical GM (A and B). In most, no or limited perilesional edema (arrow in A) was found. When gradient-echo images (T2\*, SWI) were available, signal loss was detected in about half of the cases (C). An example of nodular, leptomeningeal metastases at the foramen of Monro is shown in D (black arrow). In general, ADC values were relatively low. An example is given in E:  $ADC_{mean}$  in a ROI placed within the solid tumor component is  $660 \times 10^{-6} \text{ mm}^2/\text{s}$  ( $ADC_{minimum}$ ,  $550 \times 10^{-6} \text{ mm}^2/\text{s}$ ;  $ADC_{maximum}$ ,  $760 \times 10^{-6} \text{ mm}^2/\text{s}$ ). Contrast enhancement on T1WI was mostly mild to-intermediate compared with the choroid plexus and seen in larger parts of the solid component (F). Nonsolid tumor components with thick, irregular borders were often noted representing necrotic regions (F). The main tumor load was often located in the WM with compression (arrowhead in A) or infiltration (star in F) of the overlying cortex, or it appeared to originate from the cortex (B). Skull remodeling was detected in about half of the cases (arrow on CT in G), often associated with bony signal changes (arrowhead, H).

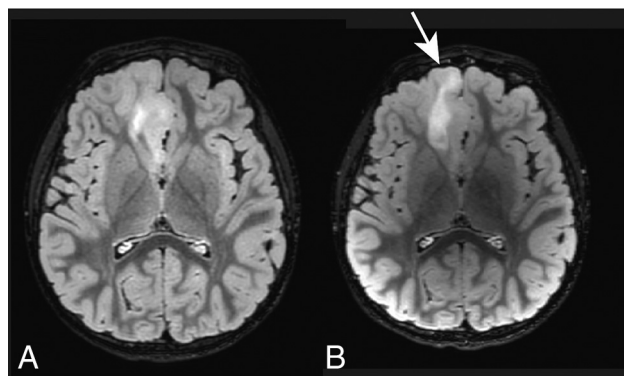


**FIG 2.** Axial FLAIR of a 4.5-year-old boy presenting with seizures. Initially, a focal cortical dysplasia of the right frontal lobe was proposed (A). The follow-up MR imaging 8 months later shows disease progression (arrow in B). After resection, the diagnosis of a CNS NB-FOXR2 was made, whereas the diagnosis of a focal cortical dysplasia was dismissed.

In all cases, the solid component was at least in some parts T2WI hyperintense compared with normal cortex but was increasingly heterogeneous in larger tumors (T2WI hyper-, iso-, and hypointense; Fig 1A, -B).

Signal loss was noted in 43% of cases with available SWI or T2\* data (Fig 1C). It was not possible to confidently determine the cause of increased susceptibility (hemorrhage versus calcification) even if phase images were available. However, in 3 patients, calcifications were unequivocally identified by CT, and in 1 patient, associated fluid levels confirmed the presence of hemorrhage on MR imaging. Altogether in 48% of cases, calcifications or hemorrhages or both were diagnosed on the basis of a combination of T1WI, T2WI, T2\*, SWI, and the  $B_0$  series of DWI data.

ADC values varied considerably between and within tumors (Fig 1D), but generally low values were probed in the solid portion, with an average  $ADC_{mean}$  of  $687.8$  (SD,  $136.3$ )  $\times 10^{-6} \text{ mm}^2/\text{s}$ .

Most tumors showed a multilobulated appearance (64%; Fig 1A-F), and 20% were multifocal. Perifocal edema was not particularly pronounced and, at most, of intermediate degree. Almost all tumors had nonsolid parts (Fig 1A, -B and E, -F) except the second smallest, which had a volume of only 10.5 mL. Unequivocal necrosis with thick, irregular, enhancing walls was diagnosed in 16% of cases (Fig 1A, -E); cysts, in 25%; and both, in another 25%.

Intracranial metastases were detected in 5 patients (20%), characterized by nodular leptomeningeal disease. One of these patients (a 4.5-year-old boy) also showed intraspinal dissemination.

High lipid and lactate peaks were noted in the enhancing part of the tumor with available MRS (single-voxel, short TE). Enhancing and nonenhancing tumor components showed a decrease in the NAA/Cr ratio (0.8 and 0.96, respectively) and an increase in Cho/NAA (3.12 and 1.74, respectively) and Cho/Cr (2.5 and 1.66, respectively) ratios. CBF was elevated on arterial spin-labeling data in the same patients.

The tumor of 1 patient, a 5-year-old boy presenting with seizures, was initially suspected to represent focal cortical dysplasia based on MR imaging findings (Fig 2A). He was treated for epilepsy under regular MR imaging surveillance. After 8 months, interval growth was noted (Fig 2B), prompting total resection. A CNS NB-FOXR2 tumor was diagnosed, whereas the diagnosis of a focal cortical dysplasia was dismissed.

## DISCUSSION

CNS NB-FOXR2 has recently been added as a tumor type in the 2021 WHO Classification of CNS tumors. Therefore, only a few case series describing its imaging features exist.<sup>6,7,10-13</sup> In our international cohort of 25 patients, we found that these were



supratentorial, often large, multilobulated tumors with little-or-no perifocal edema. Tumors nearly always showed a mix of solid and cystic/necrotic components. Involvement of the cortex was present in most cases, and the WM was involved in all patients. Lesions showed intermediate and inhomogeneous contrast enhancement and high vascularity with the presence of hemorrhage and/or calcifications. The epicenter of the tumor appeared to be in the periventricular and subcortical WM or the cortex. In almost half of the cases, the adjacent skull was remodeled with thinning of the inner table, and in some cases, pathologic signal changes in the affected bone were present. The T2WI intensity in the solid parts was heterogeneous, but always hyperintense to GM. The ADC values were relatively low but fluctuated considerably within the solid components. Multifocality and dissemination were seen, but rarely.

CNS NB-FOXR2 tumors in our cohort showed several imaging features suggesting a high-grade malignancy, such as low ADC values, large volumes, and necrosis. However, they also showed characteristics of less aggressive tumors, including relative T2WI hyperintensity, little perifocal edema, and remodeling of the skull. Imaging characteristics described in our study are not specific, and ependymoma and other embryonal tumors such as ETMR, CNS tumor with *BCOR* internal tandem duplication (CNS *BCOR*-ITD), and ATRT need to be considered in the differential diagnosis. Of these tumors, CNS NB-FOXR2 is the only type that, to the best of our knowledge, has exclusively presented in a supratentorial location, whereas the other tumor types can develop infratentorially with varying frequencies.<sup>4,10,11,13-19</sup> In addition, patient age may help with differentiation because the median age at diagnosis for patients with CNS NB-FOXR2 is 5 years (range, 1–20 years), while patients rarely present within the first 2 years of life.<sup>4</sup> In contrast, patients with ATRT are typically younger than 2 years of age, with 33% younger than 1 year of age at diagnosis.<sup>20</sup> ETMR usually presents in the first 4 years of life,<sup>4,21,22</sup> and the median age for presentation with CNS *BCOR*-ITD is 4 years (range, 0.6–22 years). The presentation age for supratentorial ependymomas is highly dependent on the molecular subtype. Supratentorial ependymoma, *YAP1* fusion-positive, occurs at a median age of 1.4 years,<sup>23</sup> while *ZFTA* fusion-positive ependymoma presents at a median age of 8 years (largely overlapping with tumors previously diagnosed as ependymoma, *RELA*-fused).<sup>23,24</sup>

The discrepancy between restricted diffusion, usually attributed to high cellularity, and high signal on T2WI that is typically seen in low-proliferative processes has previously been described in ATRT.<sup>14</sup> High cellularity is, however, only one of several causes for restricted diffusion. The microenvironment, neuropil density, cell size, or nuclear volume fraction may contribute to low ADC values, possibly without necessarily decreasing the T2WI signal.<sup>25</sup> With the current data, we are not able to specify these contributions in more detail. Skull remodeling was found in nearly half of our patients. While this is a relatively common feature in low-grade CNS tumors, we found additional calvarial signal changes in some of these cases, which has also been described at initial diagnosis in ATRT<sup>19</sup> but appears to be rare in other pediatric high-grade tumors.

Only 1 previously published case can be compared with our series<sup>7</sup> because the 2 patients described previously by Holsten et al<sup>6</sup>

are included in our cohort. However, because the focus of the case report by Furuta et al<sup>7</sup> was not primarily on imaging characteristics, the comparison remains limited. Furuta et al also found a relatively large, partially enhancing, centrally necrotic tumor with scattered calcification but, in their case, with extensive perilesional edema.

As stated previously, some of the cases we included represent a subcohort of a previously published pathology series of retrospectively re-classified CNS NB-FOXR2 tumors.<sup>4</sup> In this study of 307 tumors with an initial diagnosis of CNS-PNET, 36 (12%) were classified as CNS NB-FOXR2 by DNA methylation profiling in this series. In a pooled cohort of 63 patients with CNS NB-FOXR2, which included additionally identified cases, the 5-year progression-free survival and overall survival was 63% and 85%.<sup>4</sup> The frequency of relapses was lowest among patients treated with surgical resection and craniospinal irradiation combined with chemotherapy. This finding is in agreement with another published series that includes overlapping patients.<sup>5</sup>

We did not use the Visually AcceSable Rembrandt Images (VASARI) criteria<sup>26</sup> for our assessments because the criteria were not judged fit for our purpose, too detailed in some respects, and not pediatric-specific.

Due to the retrospective nature of our study, the imaging data were sometimes incomplete (eg, missing DWI and T2\*/SWI series). While CT images were especially helpful in verifying calcifications or bony changes, they were only available for 4 patients. In addition, advanced MR imaging may have been useful to characterize the tumors in more detail, eg, by shedding some light on neo-angiogenesis with PWI or on metabolic and microstructural changes by MRS or advanced diffusion-weighted techniques, but the multi-institutional approach and the long inclusion period of >18 years due to the rarity of these tumors precluded the availability of these imaging techniques in this study.

The integrated diagnosis of molecular and morphologic features in CNS tumor diagnostics has radically changed the classification system. The knowledge of an increasing number of molecular profiles and the revision of previous classification groups has entailed and will entail a far more detailed taxonomy. Multicenter collaboration becomes pivotal as cases become rarer, and tumor entities will have to be phenotyped through consensus reading. Our experience with weekly joint online meetings was excellent to achieve this objective.

## CONCLUSIONS

We described typical imaging characteristics of CNS NB-FOXR2 tumors in a multicenter series of 25 patients, the largest to date. Our findings contribute further to the description of new tumor types included in the 5th edition of the WHO Classification of CNS tumors. Important work lies ahead of radiologists to describe and possibly differentiate these emerging entities. Because an increasing subdivision will inevitably be accompanied by fewer cases per center, further multi-institutional reviews will be needed in the future.

## ACKNOWLEDGMENTS

We thank Magnus Sabel and Elizabeth Schepke (Queen Silvias Children's Hospital, Sahlgrenska University Hospital, Gothenburg, Sweden), Stefan Rutkowski (Department of Paediatric Haematology

and Oncology, University Medical Centre Hamburg-Eppendorf, Hamburg, Germany), Barbara von Zezschwitz (Department of Pediatric Oncology and Hematology, Charité–Universitätsmedizin Berlin, Germany), Darren Hargrave (Pediatric Oncology Unit, UCL Great Ormond Street Institute of Child Health, London, UK), Tom Jacques (Developmental Biology and Cancer Research & Teaching Department, UCL Great Ormond Street Institute of Child Health, London, UK), and Pieter Wesseling (Department of Pathology, Amsterdam University Medical Centers/VU Medisch Centrum, Amsterdam, the Netherlands) for contributing clinical and molecular data. All research at Great Ormond Street Hospital NHS Foundation Trust and UCL Great Ormond Street Institute of Child Health is made possible by the NIHR Great Ormond Street Hospital Biomedical Research Centre. The views expressed are those of the author(s) and not necessarily those of the NHS, the NIHR or the Department of Health.

**Disclosure forms** provided by the authors are available with the full text and PDF of this article at [www.ajnr.org](http://www.ajnr.org).

## REFERENCES

- Louis DN, Perry A, Wesseling P, et al. **The 2021 WHO Classification of Tumors of the Central Nervous System: a summary.** *Neuro Oncol* 2021;23:1231–51 [CrossRef Medline](#)
- Louis DN, Ohgaki H, Wiestler OD, et al. **The 2007 WHO classification of tumours of the central nervous system.** *Acta Neuropathol* 2007;114:97–109 [CrossRef Medline](#)
- Sturm D, Orr BA, Toprak UH, et al. **New brain tumor entities emerge from molecular classification of CNS-PNETs.** *Cell* 2016; 164:1060–72 [CrossRef Medline](#)
- von Hoff K, Haberler C, Schmitt-Hoffner F, et al. **Therapeutic implications of improved molecular diagnostics for rare CNS embryonal tumor entities: results of an international, retrospective study.** *Neuro Oncol* 2021;23:1597–611 [CrossRef Medline](#)
- Korshunov A, Okonechnikov K, Schmitt-Hoffner F, et al. **Molecular analysis of pediatric CNS-PNET revealed nosologic heterogeneity and potent diagnostic markers for CNS neuroblastoma with FOXR2-activation.** *Acta Neuropathol Commun* 2021;9:20 [CrossRef Medline](#)
- Holsten T, Lubieniecki F, Spohn M, et al. **Detailed clinical and histopathological description of 8 cases of molecularly defined CNS neuroblastomas.** *J Neuropathol Exp Neurol* 2021;80:52–59 [CrossRef Medline](#)
- Furuta T, Moritsubo M, Muta H, et al. **Central nervous system neuroblastoma with FOXR2 activation presenting both neuronal and glial differentiation: a case report.** *Brain Tumor Pathol* 2020; 37:100–104 [CrossRef Medline](#)
- Capper D, Jones DTW, Sill M, et al. **DNA methylation-based classification of central nervous system tumours.** *Nature* 2018;555:469–74 [CrossRef Medline](#)
- Stock A, Mynarek M, Pietsch T, et al. **Characteristics of wingless pathway subgroup medulloblastomas: results from the German Imaging HIT/SIOP-Trial Cohort.** *AJNR Am J Neuroradiol* 2019; 40:1811–17 [CrossRef Medline](#)
- Ferris SP, Velazquez Vega J, Aboian M, et al. **High-grade neuroepithelial tumor with BCOR exon 15 internal tandem duplication: a comprehensive clinical, radiographic, pathologic, and genomic analysis.** *Brain Pathol* 2020;30:46–62 [CrossRef Medline](#)
- De Lima L, Sürme MB, Gessi M, et al. **Central nervous system high-grade neuroepithelial tumor with BCOR alteration (CNS HGNET-BCOR): case-based reviews.** *Childs Nerv Syst* 2020;36:1589–99 [CrossRef Medline](#)
- Hu W, Wang J, Yuan L, et al. **Case report: a unique case of pediatric central nervous system embryonal tumor harboring the CIC-LEUTX fusion, germline NBN variant and somatic TSC2 mutation: expanding the spectrum of CIC-rearranged neoplasia.** *Front Oncol* 2020;10:598970 [CrossRef Medline](#)
- Cardoen L, Tauziède-Espariat A, Dangouloff-Ros V, et al. **Imaging features with histopathologic correlation of CNS high-grade neuroepithelial tumors with a BCOR internal tandem duplication.** *AJNR Am J Neuroradiol* 2022;43:151–56 [CrossRef Medline](#)
- Jin B, Feng XY. **MRI features of atypical teratoid/rhabdoid tumors in children.** *Pediatr Radiology* 2013;43:1001–08 [CrossRef Medline](#)
- Meyers SP, Khademian ZP, Biegel JA, et al. **Primary intracranial atypical teratoid/rhabdoid tumors of infancy and childhood: MRI features and patient outcomes.** *AJNR Am J Neuroradiol* 2006; 27:962–71 [Medline](#)
- Yamasaki K, Kiyotani C, Terashima K, et al. **Clinical characteristics, treatment, and survival outcome in pediatric patients with atypical teratoid/rhabdoid tumors: a retrospective study by the Japan Children's Cancer Group.** *J Neurosurg Pediatr* 2019;15:1–10 [CrossRef Medline](#)
- Mangalore S, Aryan S, Prasad C, et al. **Imaging characteristics of supratentorial ependymomas: study on a large single institutional cohort with histopathological correlation.** *Asian J Neurosurg* 2015;10:276–81 [CrossRef Medline](#)
- Wang Q, Cheng J, Li J, et al. **The survival and prognostic factors of supratentorial cortical ependymomas: a retrospective cohort study and literature-based analysis.** *Front Oncol* 2020;10:1585 [CrossRef Medline](#)
- Warmuth-Metz M, Bison B, Gerber NU, et al. **Bone involvement in atypical teratoid/rhabdoid tumors of the CNS.** *AJNR Am J Neuroradiol* 2013;34:2039–42 [CrossRef Medline](#)
- WHO Classification of Tumours Editorial Board. *Central Nervous System Tumours: WHO Classification of Tumours*. 5th ed. International Agency for Research on Cancer; December 2021
- Frühwald MC, Hasselblatt M, Nemes K, et al. **Age and DNA methylation subgroup as potential independent risk factors for treatment stratification in children with atypical teratoid/rhabdoid tumors.** *Neuro Oncol* 2020;22:1006–17 [CrossRef Medline](#)
- Khan S, Solano-Paez P, Suwal T, et al. **Clinical phenotypes and prognostic features of embryonal tumours with multi-layered rosettes: a Rare Brain Tumor Registry study.** *Lancet Child Adolesc Health* 2021;5:800–13 [CrossRef Medline](#)
- Pajtler KW, Witt H, Sill M, et al. **Molecular classification of ependymal tumors across all CNS compartments, histopathological grades, and age groups.** *Cancer Cell* 2015;27:728–43 [CrossRef Medline](#)
- Andreioulo F, Varlet P, Tauziède-Espariat A, et al. **Childhood supratentorial ependymomas with YAP1-MAML1 fusion: an entity with characteristic clinical, radiological, cytogenetic and histopathological features.** *Brain Pathol* 2019;29:205–16 [CrossRef Medline](#)
- Maier SE, Sun Y, Mulkern RV. **Diffusion imaging of brain tumors.** *NMR Biomed* 2010;23:849–64 [CrossRef Medline](#)
- VASARI Research Project. March 30, 2020. <https://wiki.cancerimagingarchive.net/display/Public/VASARI+Research+Project>. Accessed May 29, 2022